



This is a repository copy of *IGBT Thermal Stress Reduction Using Advance Control Strategy*.

White Rose Research Online URL for this paper:
<http://eprints.whiterose.ac.uk/134141/>

Version: Published Version

Article:

Soulatiantork, P. orcid.org/0000-0003-3212-8220, Alghassi, A., Faifer, M. et al. (1 more author) (2017) IGBT Thermal Stress Reduction Using Advance Control Strategy. *Procedia CIRP*, 59. pp. 274-279. ISSN 2212-8271

<https://doi.org/10.1016/j.procir.2016.09.040>

Reuse

This article is distributed under the terms of the Creative Commons Attribution-NonCommercial-NoDerivs (CC BY-NC-ND) licence. This licence only allows you to download this work and share it with others as long as you credit the authors, but you can't change the article in any way or use it commercially. More information and the full terms of the licence here: <https://creativecommons.org/licenses/>

Takedown

If you consider content in White Rose Research Online to be in breach of UK law, please notify us by emailing eprints@whiterose.ac.uk including the URL of the record and the reason for the withdrawal request.



eprints@whiterose.ac.uk
<https://eprints.whiterose.ac.uk/>

The 5th International Conference on Through-life Engineering Services (TESConf 2016)

IGBT Thermal Stress Reduction Using Advance Control Strategy

Payam Soulatiantork¹*, Alireza Alghassi², Marco Faifer³, Suresh Perinpanayagam²

¹Energy Department, Politecnico di Milano, Milano, Italy

²School of Aerospace, Transport and Manufacturing, Cranfield University, Bedford MK43 0AL, UK

³DEIB, Politecnico di Milano, Milano, Italy

* E-mail address: Payam.soulatiantork@polimi.it.

Abstract

Next-generation advances in stress control strategy will enable renewable energies, such as solar energy, to become more reliable and available. Critical components, such as power electronics, present uncertainties to the system control in malfunctioning process, which reduces the target of more clean energy development and CO₂ emission reduction. Thus, developing and harnessing sustainable energy requires mitigating the impact of the variability of the source of energy and the impact of the adaptive stress control deployed for the proportional, integral, derivative (PID) controller to minimize the thermal stress in the power switch insulated gate bipolar transistor (IGBT). In response to this challenge, a fuzzy linear matrix inequality (FLMI) PID controller proposes initiatives for customizing parameters of PID controller corresponding to the uncertainty of IGBTs. In this paper, the uncertainty of the boost converter has been evaluated in the dynamic of the LMI model and Takagi-Sugino (TS) has applied in closed loop control to overcome the instability of the Boost converter parameters.

© 2016 The Authors. Published by Elsevier B.V. This is an open access article under the CC BY-NC-ND license (<http://creativecommons.org/licenses/by-nc-nd/4.0/>).

Peer-review under responsibility of the scientific committee of the The 5th International Conference on Through-life Engineering Services (TESConf 2016)

Keywords: Power Electronic Converter, EV, IGBT, Conditional Base Monitoring (CBM), PID Controller, FLMI

I. Introduction

A stringent control design approach to monitoring the power switches' degradation process leads industries to advance adapting health management to coincide with operational conditions. Semiconductor insulated gate bipolar transistor (IGBT) are subjected to an extensive heat generation from junction due to high operation voltage. The problem of components overheating becomes critical when systems such as Photovoltaic (PV) ones are taken into account. In fact, these systems can be placed in high-temperature environment, increasing significantly the vulnerability of the power modules to thermal fatigue. In the IGBT package structure, the heat path conduction can change over the life span due to crack growth in weak parts of the packaging structure (e.g. solder joint). These phenomena can cause a thermal runaway of the device [1]. The IGBT failure mechanisms, such as solder joint crack and wire bond joint lift off,

accelerate due to aging process caused by high-temperature variation stress, thus reducing the device life reliability. For IGBTs, parameters used as precursors to monitor abnormality performance include on-state collector-emitter voltage ($V_{ce(on)}$), collector-emitter leakage current (I_{ce}), on-resistance (R_{ce}) and gate emitter voltage threshold ($V_{ge(th)}$) [2]. This paper aims to develop a robust algorithm to minimize thermal stress swings caused by degradation of the device. The proposed algorithm reconfigures the current reference at as such that PID controller adapts itself as quickly as possible of the failure detection (ideally, less than 10 μ s) to produce desire duty cycle (D) for PWM generator to avoid expediency of failure propagation. Therefore, a versatile control approach has a considerable interest for reducing drawn power modules in degradation process. In order to design the proposed PID controller using FLMI technique for boost converter, the state space average

model of the boost DC-DC converter has been used. This model aims to define the uncertain parameters, which are the duty cycle and the PV panel voltage. Defined parameters interval will be used in the design of proposed PID controller parameters ($K_p, K_i,$ and K_d). In addition, due to variation of the input voltage, the uncertainty bound is defined around the power supply input voltage within the PID controller using the fuzzy linear matrix inequalities (FLMI) technique to create optimized Proportional, Integral, and Derivative (PID) (i.e. ($K_p, K_i,$ and K_d)) parameters. Furthermore, duty cycle complimentary (1-D) is also considered as an uncertainty in the FLMI technique. The large thermal stress variation is the main factor that overrides IGBT's packaging structure connections, such as the bond wire connection, die-attached solder and substrate solder joint, and effectively reduces the IGBT's life span. The novel idea is to decelerate the trend of the junction temperature slope when the abnormality is detected using the ($V_{ce(on)}$) parameter as an indication of the bond wire lift-off. This will result in relieving the stress level and accordingly improving the IGBT's lifetime expectancy, in overall increasing DC-DC boost converter lifetime [3]. The thermal stress reduction management strategy depends on estimation junction temperature and feedback PV reference current. The PID controller is directly fed with an updated I_{ref} that is set by thermal stress reduction control according to rising up temperature variation slope (see Fig. 1) [4].

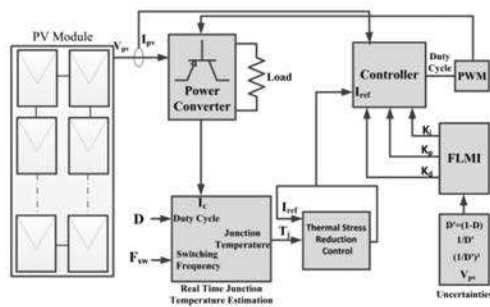


Fig. 1. Proposed schematic diagram of sensorless thermal stress reduction control.

The FLMI control approach is coinciding with time to failure detection and improves convergence speed as the temperature swing rise up. Overall, PV system availability has increased considerably during downtime since the power converter encounters less thermal stress change.

II. Thermal Stress Reduction Control

Thermal stress reduction control (TSRC) illustrated in Fig. 2 is used to reduce stress factor of junction temperature (T_j) variation rise up which has progressed due to failure mechanisms propagation such as wire bond lift-off, aluminium metallization reconstruction [5]. Changeable parameters, like duty cycle, can be varied by monitoring T_j and accordingly adjusting the input current reference (I_{ref})

received from the MPPT to desired value, according to severity of thermal stress. The baseline for assessing the boundary of duty cycle is necessary to use for well establishing in FLMI. Using the uncertainty parameter is to facilitate the PID controller with reliable parameters in order to necessitate immediate response to time to failure injection. The active TSRC proposed for minimising thermal stress enhances the robustness of the PID controller by updating I_{ref} . As the failure mode of the IGBT is temperature variation dependent, it is important to estimate T_j which can indicate the average temperature of the device in different operating conditions. Hence, the prediction of the precise T_j is performed using the RMS value of the switch current during on and off switching mode injecting to the pre-defined look-up table of energy losses at different interpolation of temperatures. Thus, to include all these dependencies, the overall power losses superimposes to real-time electro-thermal model which assembles from thermal material parameters (R_{th}, C_{th}) of the IGBT to reach the desired online T_j estimation [6]. The relationship between a change in the slope of T_j and a change in I_{ref} is approximated. In turn, a change in the duty cycle and a change in the output current can be determined to reduce the slope of the thermal stress. In such wire bond lift-off phenomena, the control schema may to adjust the duty cycle of switch by an amount ΔI_{ref} in accordance with slope of T_j begins to increase at junction temperature reference (T_{jref}) and accordingly this arrangement feeds the IGBT driver. In this paper, failure mechanisms are emulated in similar fashion to the solder fatigue. This has been done at two different times in simulation ($t=0.03s, t=0.1s$) to validate the robustness of FLMI. In both conditions, T_j ramps up with slope $k=40$ °C/s and exceeds above the safety margin value (e.g. 70°C). The failure rate will be higher in high temperature variation. Therefore, the proposed TSRC intervenes with the appropriate remedial action when the estimated T_j may reach values of 70 °C corresponding to normal operating conditions, and more to mitigate the impending failure. The long-term reliability of the converter is dependent on minimizing the failure rate, which needs a response in much shorter amount of time. The purpose of the FLMI is exploited to determine parameters in active failure operating region to allow duty cycle regulated in considered uncertainty boundary conditions and reach to steady state faster, which improves IGBT performance to operate in downtime longer at the time of failure progression and consequently increases converter lifespan. It can be noted, the parameters are tuned rigorously which decelerates the slope junction temperature rising above 70 °C as the I_{ref} updated within steady state region of the maintained duty cycle almost 0.9 at effective switching frequency (f_{sw}) rate 10kHz of the IGBT.

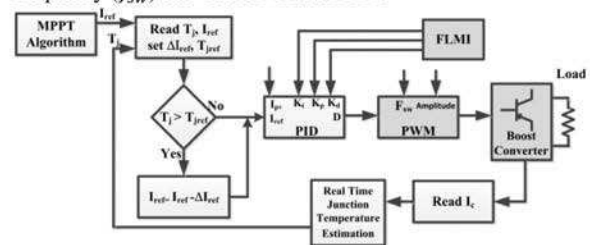


Fig. 2. Thermal stress reduction control strategy.

III. State Space Representation and Uncertainties in Boost Converter

A schematic circuit diagram of a boost converter is provided in Fig. 3. The load resistor models the converter load, whilst C2, L and D represent the capacitor, the inductor, and the diode, respectively. C1 is used to prevent impedance interactions with input supply.

Pulse width modulation (PWM) is used to control the gate of the IGBT.

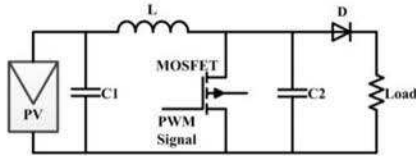


Fig. 3. Boost DC-DC converter

For a boost converter, the state space averaged model can be written as,

$$\begin{cases} \dot{x}(t) = Ax(t) + B_w w(t) + B_u u(t) + B_{ref} V_{ref} \\ z(t) = C_z x(t) + D_{zw} w(t) + D_{zu} u(t) \end{cases} \quad (1)$$

Where $A \in \mathbb{R}^{n \times n}, B_w \in \mathbb{R}^{n \times r}, B_u \in \mathbb{R}^{n \times m}, C_z \in \mathbb{R}^{p \times n}, D_{zw} \in \mathbb{R}^{p \times r}, D_{zu} \in \mathbb{R}^{p \times m}$

$$x(t) = \begin{bmatrix} i_L(t) \\ v_o(t) \\ x_3(t) \end{bmatrix}, \quad w(t) = [i_{load}(t)], \quad u(t) = [d_a(t)],$$

$$z(t) = [v_o(t)]$$

i_L is the photovoltaic panel current and v_o is the output voltage. The third state variable is x_3 , which is the integral of the error signal obtained from the difference between the reference current I_{ref} and the input current I_i . It is clear that x_3 is constant because at the equilibrium state, the current error is zero. Vector w is the disturbance vector due to characterize the output impedance. The matrices of the state-space can be represented as;

$$\begin{aligned} A &= \begin{bmatrix} 0 & -\frac{D'_d}{L} & 0 \\ \frac{D'_d}{C} & -\frac{1}{RC} & 0 \\ 0 & -1 & 0 \end{bmatrix}, B_w = \begin{bmatrix} 0 \\ 0 \\ 0 \end{bmatrix}, \\ B_u &= \begin{bmatrix} \frac{V'_i}{D'_d L} \\ \frac{V_i}{(D'_d R)C} \\ 0 \end{bmatrix}, B_{ref} = \begin{bmatrix} 0 \\ 0 \\ 1 \end{bmatrix}, \\ C_z &= [0 \quad 1 \quad 0], D_{zw} = [0], D_{zu} = [0] \end{aligned} \quad (2)$$

Where D'_d is the complementary of the duty cycle operating point duty cycle D_d .

In addition to previously-considered parameters, the duty cycle, $D'_d (1 - D_d)$, $1/D'_d$ and $1/D'^2_d$ as uncertain and time-varying parameters, in this paper we have considered the input voltage of the converter which is the photovoltaic panel voltage as a new uncertain parameter because the voltage of photovoltaic panels change during day time and variations in environmental conditions. Two new parameters, δ and β , must be defined because the matrices are not linearly

dependent on the uncertain parameters D'_d and D'^2_d in order to meet with a linear dependence. Using new parameter vectors, which are, D'_d, δ, β , and V_i , the uncertainty can be bounded inside a convex polytope [7].

As the formulated uncertainty model given in last part, the aim is to find a state feedback gain $K (u=Kx)$, where uncertainty is restricted within the intervals given below,

$$\begin{aligned} V_{pv} &\in [V_{pv.min}, V_{pv.max}] \\ \delta &\in [1/D'_{dmax}, 1/D'_{dmin}] \\ \beta &\in [1/D'^2_{dmax}, 1/D'^2_{dmin}] \\ D'_d &\in [D'_{dmin}, D'_{dmax}] \end{aligned}$$

As the converter matrices A and B_u have different states, the objective of the design must guarantee the reduction in level of the perturbation rejection in all states.

IV. FLMI Design Constraints

TSRC strategy has to manipulate with I_{ref} in malfunction region, where is needed to deploy uncertain parameters in order to build up robust PID controller to standby in remedial action. As a result, the FLMI PID controller has been proposed to establish interval uncertainty parameters to mitigate the stress level by adjusting the duty cycle. The dynamic average model of the boost converter is bilinear since $A_{on} \neq A_{off}$ and can be written as,

$$\dot{\hat{x}} = A\hat{x} + B_u(\hat{x})\hat{d} \quad (3)$$

where \hat{x} and \hat{d} are the perturbed values of the states and the duty cycle around the equilibrium points. Matrix A can be written as:

$$A = \begin{bmatrix} 0 & -\frac{D'_d}{L} & 0 \\ \frac{D'_d}{C} & -\frac{1}{RC} & 0 \\ 0 & -1 & 0 \end{bmatrix}, B_u(\hat{x}) = \begin{bmatrix} \frac{V_g}{D'_d L} + \frac{\hat{v}_{c2}(t)}{L} \\ \frac{V_g}{(D'^2_d R)C} - \frac{\hat{i}_L(t)}{C} \\ 0 \end{bmatrix}$$

Between two most useful approaches to fuzzy representations, the Takagi- Sugeno approach has been used in this paper because the dynamic model of the converter is known.

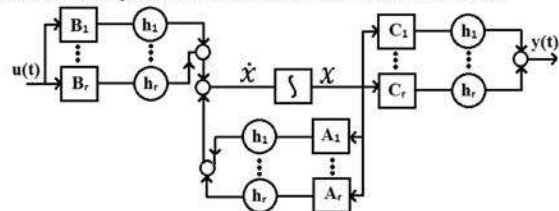


Fig. 4. Nonlinear plant as a group of linear models

For a group of linear models, the model of the nonlinear plant is depicted in Fig. 4, which represents the relationship between the input and the output of the system as described below,

$$\begin{aligned} R_i &= \text{If } \delta_1 \text{ is } M_{i1} \text{ and } \dots \text{ and } \delta_j \text{ is } M_{ji} \text{ then} \\ \dot{x}_i(t) &= A_i x(t) + B_i u(t) \quad i = 1, 2, \dots, r \end{aligned} \quad (4)$$

Where $x(t)$ is the vector of the state space, $u(t)$ is the vector of inputs, M_{ji} are the fuzzy sets r is the number of models [8]-[9].

The entire fuzzy model of the plant corresponds to a fuzzy weighting of the locally-valid linear submodel associated with each implication R_i .

$$\dot{x}(t) = \frac{\sum_{i=1}^r w_i(\delta(t)) [A_i x(t) + B_i u(t)]}{\sum_{i=1}^r w_i(\delta(t))} \quad (5)$$

Weights $w_i(\delta(t))$ are zero or positive time-variant values and the sum of all the weights is positive.

$$\sum_{i=1}^r w_i(\delta(t)) > 0, w_i(\delta(t)) \geq 0 \quad \forall i = 1, 2, \dots, r \quad (6)$$

Therefore, the fuzzy model with normalized weights can be written as

$$\dot{x}(t) = \sum_{i=1}^r h_i(\delta(t)) [A_i x(t) + B_i u(t)] \quad (7)$$

Matrix A is unique and described in Eq. (3) and B_i is described as

$$B_1 = \begin{bmatrix} \frac{V_g + v_{min}}{D'L + L} \\ \frac{V_g}{(D'^2R)C} \\ 0 \end{bmatrix}, B_2 = \begin{bmatrix} \frac{V_g + v_{min}}{D'L + L} \\ \frac{V_g}{(D'^2R)C} \\ 0 \end{bmatrix} \quad (8)$$

$$B_3 = \begin{bmatrix} \frac{V_g + v_{max}}{D'L + L} \\ \frac{V_g}{(D'^2R)C} \\ 0 \end{bmatrix}, B_4 = \begin{bmatrix} \frac{V_g + v_{max}}{D'L + L} \\ \frac{V_g}{(D'^2R)C} \\ 0 \end{bmatrix}$$

Being the membership function of the fuzzy sets i_{small} , i_{big} , v_{small} and v_{big} the following ones,

$$\eta_{i_{small}}(i_L) = \frac{i_{max} - i_L}{i_{max} - i_{min}}, \quad \eta_{v_{small}}(\hat{v}_C) = \frac{v_{max} - \hat{v}_C}{v_{max} - v_{min}} \quad (9)$$

$\eta_{i_{big}}(i_L)$ and $\eta_{v_{big}}(\hat{v}_C)$ are the complimentary of $\eta_{i_{small}}(i_L)$ and $\eta_{v_{small}}(\hat{v}_C)$, respectively. Thus, the normalized weight functions are

$$h_1(i_L, \hat{v}_C) = \eta_{i_{small}} \eta_{v_{small}} \quad h_2(i_L, \hat{v}_C) = \eta_{i_{small}} \eta_{v_{big}} \quad (10)$$

$$h_3(i_L, \hat{v}_C) = \eta_{i_{big}} \eta_{v_{small}} \quad h_4(i_L, \hat{v}_C) = \eta_{i_{big}} \eta_{v_{big}}$$

Therefore, the entire fuzzy converter model corresponds to

$$\dot{\hat{x}} = \sum_{i=1}^r h_i(i_L, \hat{v}_C) (A_i x(t) + B_i \hat{d}(t)) \quad (11)$$

As mentioned before the normalized weight summation of all the $h_i(\delta(t))=1$ and A is unique the fuzzy converter model can be described as

$$\dot{\hat{x}} = A \hat{x} + (\sum_{i=1}^r h_i(i_L, \hat{v}_C) B_i) \hat{d}(t) \quad (12)$$

Therefore, the controller rule must be as follows in, which F_i are vectors of linear feedback gain of each rule,

$$R_i: \text{ If } \delta_1 \text{ is } M_{i1} \text{ and ... and } \delta_j \text{ is } M_{ji} \text{ Then } u(t) = F_i x(t) \quad i = 1, \dots, r \quad (13)$$

The entire fuzzy controller can be written as

$$u(t) = - \frac{\sum_{i=1}^r w_i F_i x(t)}{\sum_{i=1}^r w_i} = - \sum_{i=1}^r h_i F_i x(t) \quad (14)$$

Substituting the control law of Eq. (13) in the fuzzy model described in Eq. (14), the closed loop system dynamics is given by

$$\dot{x}(t) = \sum_{i=1}^r \sum_{j=1}^r h_i h_j (A_i - B_i F_j) x(t) \quad (15)$$

The continuous fuzzy system is quadratically stable for some feedback gain F_i if there exists a common positive definite matrix W such that

$$A_i W + W A_i^T - B_i Y_i - Y_i^T B_i^T < 0 \quad i=1, \dots, r$$

$$A_i W + W A_i^T + A_j W + W A_j^T - B_i Y_j - Y_j^T B_i^T - B_j Y_i - Y_i^T B_j^T \leq 0, i < j \leq r \quad (16)$$

In order to have a better transient performance in the closed loop system, the poles must be in a region, which expressed in terms of decay rate. Therefore, the linear matrix inequalities would be

$$A_i W + W A_i^T - B_i Y_i - Y_i^T B_i^T + 2 \alpha W < 0, \quad i = 1, \dots, r$$

$$A_i W + W A_i^T + A_j W + W A_j^T - B_i Y_j - Y_j^T B_i^T - B_j Y_i - Y_i^T B_j^T + 4 \alpha W \leq 0, i < j \leq r \quad (17)$$

According to the above section, the objective is to find the matrices W and Y by maximizing α with solving above inequalities [8]-[9].

By finding these two matrices, the feedback gain K can be defined as

$$K = YW^{-1} \quad (18)$$

The following section discusses the design of a state space feedback PID controller in order to find the K_p , K_i and K_d parameters by using the feedback gain (K) calculated above [10].

V. State Feedback PID Control Design

The idea is to find the PID parameters based on fuzzy LMI feedback gain calculated before. The algorithm output must be a reference for PID, which is tuned by the fuzzy LMI technique. In addition of conventional PID tuners, fuzzy LMI is a technique to tune the K_p , K_i and K_d parameters [11].

The PID controller state feedback can be described as

$$d(t) = K_i \int (I_{ref} - I_i) dt + K_p (I_{ref} - I_i) + K_d \frac{d(I_{ref} - I_i)}{dt} \quad (19)$$

Where I_{ref} is the MPPT algorithm output and I_i is the photovoltaic panel current, which should be controlled. In addition to the two state space variables in the boost converter, which are I_L (inductor current) and V_{C2} (C2 voltage), the error is defined as the third state of the system.

$$z \equiv \int (I_{ref} - I_{out}) dt \quad (20)$$

Therefore, the new state vector would be

$$Z = \begin{bmatrix} x \\ z \end{bmatrix} \tag{21}$$

By combining Equations (19) and (20),

$$d = k_i z - k_p Cx - k_d C\dot{x} + k_p I_{ref} \tag{22}$$

$$d = -(I + k_d CB_d)^{-1} (k_p C + k_d CA_d)x + (I + K_d CB_d)^{-1} k_i z + (I + k_d CB_d)^{-1} k_p I_{ref} \tag{23}$$

Therefore, the controller equation, which can expressed as state feedback $d = K_a Z$ is

$$d = (I + k_d CB_d)^{-1} [-(k_p C + k_d CA_d) \ k_i] Z + (I + k_d CB_d)^{-1} k_p I_{ref} \tag{24}$$

The final representation of the augmented system may be written as

$$\dot{Z} = \begin{bmatrix} A_d & 0 \\ -C & 0 \end{bmatrix} Z + \begin{bmatrix} B_d \\ 0 \end{bmatrix} d + \begin{bmatrix} 0 \\ I_{ref} \end{bmatrix} \tag{25}$$

$$V_0 = [C \ 0]Z$$

where, $d = K_a Z$

By comparing d with the gain calculated by the fuzzy LMI in the previous section, PID parameters can be obtained. Disturbance rejection can be achieved by using this controller, which is designed with the fuzzy LMI approach.

VI. Simulation Results and Discussion

A photovoltaic panel has been used as the supply for the boost converter and four parameters have been considered as the uncertainties. The most crucial parameter is the PV panel voltage, which changes during the day. Thus, the proposed PID controller has the ability to work in the uncertainty intervals. The TSRC imposes on the mean operating estimated temperature to halt the over-temperature over 0.6 sec simulation run in MATLAB Simulink domain by exploiting the new PID performance.

Possible uncertainty interval parameters, such as V_{pv} and D'_d , are given in Table 1 which also includes boost converter components parameters.

Table 1. Component and uncertainty values used for simulation

V_g	(10-300) V
L	4e-3 H
$C2$	100e-7 F
Load	200Ω
D'_d	(0.2-0.95)
T_s	20e-6 s
α	110

In addition, minimizing ΔT_j improves the lifetime of the IGBT in real-time service during crack initiation at the

vicinity of the solder joint due to stress aggregation result in high temperature variation. A comparison is then done between the proposed PID and a conventional PI controller designed in reference [12]. First, according to Eq.3, Eq.8 and Table 1, the fuzzy model for boost converter would be:

$$A_1 = A_2 = A_3 = A_4 = A = \begin{bmatrix} 0 & 125 & 0 \\ 5000 & -500 & 0 \\ 0 & -1 & 0 \end{bmatrix}$$

$$B_1 = \begin{bmatrix} 55000 \\ -220000 \\ 0 \end{bmatrix} \quad B_2 = \begin{bmatrix} 55000 \\ -2220000 \\ 0 \end{bmatrix}$$

$$B_3 = \begin{bmatrix} 57500 \\ -220000 \\ 0 \end{bmatrix} \quad B_4 = \begin{bmatrix} 57500 \\ -2220000 \\ 0 \end{bmatrix}$$

Where A and B are the state space matrices of the boost converter. By choosing \hat{i}_L and \hat{v}_C from Eq. (9) the normalized weight functions are

$$h_1(\hat{i}_L, \hat{v}_C) = 0.392 \quad h_3(\hat{i}_L, \hat{v}_C) = 0.364$$

$$h_2(\hat{i}_L, \hat{v}_C) = 0.128 \quad h_4(\hat{i}_L, \hat{v}_C) = 0.115$$

The objective here is to find Y and W matrices from Eq. (16) and then the controller gains $K1$ to $K4$. Therefore, the gains have been calculated as

$$K1 = [-0.245 \quad -0.0024 \quad 18.491]$$

$$K2 = [-0.1128 \quad -0.0011 \quad 8.515]$$

$$K3 = [-0.241 \quad -0.0023 \quad 18.204]$$

$$K4 = [-0.107 \quad -0.0011 \quad 8.117]$$

Each calculated gain must be multiplied by its corresponding weight. Thus,

$$h_1 K1 + h_2 K2 + h_3 K3 + h_4 K4 = K$$

The total gain K would be, $K = [-0.2108 \quad -0.0021 \quad 15.946]$

On the other hand, in Section V, we have designed a state space feedback controller by setting this expression and the gains found by the FLMI technique in equivalence relation, which the PID parameter gains calculated as follows:

$$\begin{bmatrix} (I + k_d C_z B)^{-1} [-(k_p C_z + k_d C_z A) \ k_i] \\ \equiv [-0.2108 \quad -0.0021 \quad 15.946] \end{bmatrix}$$

Then,

$$k_p = 0.002483 \quad k_d = 3.7e - 6 \quad k_i = 3.66$$

Fig. 5 shows that proposed PID controller significantly minimizes the error to adjust the duty cycle extremely rapidly to reach a steady state when failure injected at 30 ms whereas the conventional PID controller responses relatively slowly and reaches steady state at 40 ms. Based on this approach, the TSRC incorporates with the FLMI PID controller in an appropriate time where the variable I_{ref} from MPPT algorithm can be adapted with failure injection to prevent sudden failure occurring in the IGBT. Fig. 6 depicts the slope of T_j controlled at 40°C/s and successfully has been decelerated within the boundary of the PV module voltage supply.

It is observed that immediately after failure mode injection at 100 ms junction temperatures cannot overshoot the nominal value and ensuring IGBT works in its safe margin operating condition. Furthermore, the results indicate that with the FLMI PID controller, see blue colour in Fig.6 and Fig.7 a few degree Celsius temperatures have been reduced in comparison with the conventional PID controller illustrates in red colour. The proposed PID controller dynamically improves the compatibility of TSRC for reducing thermal stress in the high-temperature region, which has a rapid adjustment of thermal stress whereas the conventional PID is involved in slower fashion with more disturbances to similarly suppress the stress level in failure region.

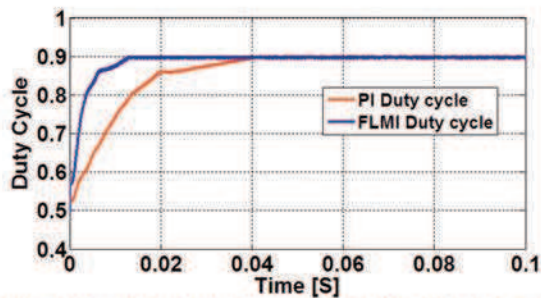


Fig. 5. Duty cycle adjustment for two different control approaches.

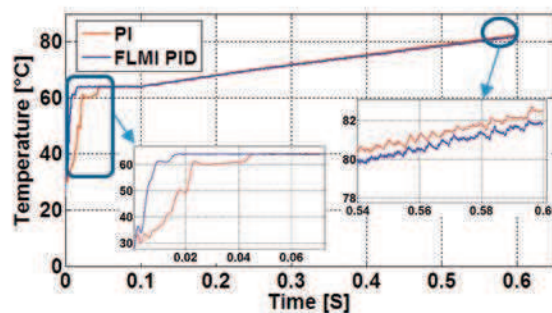


Fig. 6. Thermal stress reduction at a time to failure 0.1 s.

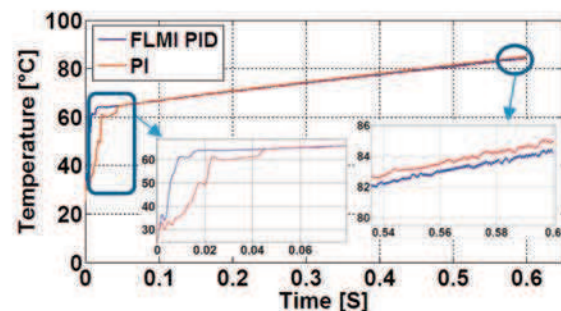


Fig. 7. Thermal stress reduction at a time to failure 0.03 s.

VII. Conclusion

This paper implements the thermal stress reduction strategy enhanced with an FLMI PID controller, which can improve the reliability of the PV system in downtime. The uncertainties of the PV voltage and the duty cycle have been taken into account so that the TSRC topology becomes more

adaptive to reconfigure the reference current of the MPPT for feeding the proposed PID controller. The proposed PID has been compared with a conventional PID controller. The results have shown that the control strategy reached steady state remarkably quickly before the IGBT progressed to the failure region. The junction temperature variation is no longer in rapid progression and the slope of T_j has kept at constant value of 40 °C/s. The duty cycle as an important parameter in the control approach has been adjusted in accordance with the propagation of the failure mode which has been induced in two different time series, 30ms and 100ms, which have shown that the new PID controller rapidly adapted to remedial region whereas the conventional has disturbance and latency to keep up with TSRC control strategy. As it can be seen from Fig.6 and Fig.7, the TSRC algorithm has a faster dynamic response at about 0.02s whereas the conventional PID controller has responded in 0.04s. In addition, in the steady state, the temperature obtained by the proposed algorithm has lower value by 0.5°C. This paper presents an advanced control strategy based on junction temperature variation to decelerate stress conditions, which improves the lifespan of the converter during failure conditions.

References

- [1] M. S. Nasrin and F. H. Khan, "Characterization of aging process in power converters using spread spectrum time domain reflectometry," *Energy Conversion Congress and Exposition (ECCE)*, 2012 IEEE, pp. 2142-2148, 2012.
- [2] N. Patil, D. Das, K. Goebel and M. Pecht, "Identification of failure precursor parameters for insulated gate bipolar transistors (IGBTs)," in *Prognostics and Health Management, PHM 2008 International Conference*, pp. 1-5, 2008.
- [3] M. Andresen and M. Liserre, "Impact of active thermal management on power electronics design," *Microelectronics Reliability*, vol. 54, pp. 1935-1939, 2014.
- [4] D. A. Murdock, J. E. R. Torres, J. J. Connors and R. D. Lorenz, "Active thermal control of power electronic modules," *Industry Applications, IEEE Transactions on*, vol. 42, pp. 552-558, 2006.
- [5] M. Ciappa, "Selected failure mechanisms of modern power modules," *Microelectronics Reliability*, vol. 42, pp. 653-667, 2002.
- [6] M. Musallam, C. M. Johnson, Chunyan Yin, C. Bailey and M. Mermet-Guyennet, "Real-time life consumption power modules prognosis using on-line rainflow algorithm in metro applications," *Energy Conversion Congress and Exposition (ECCE)*, 2010 IEEE, pp. 970-977, 2010.
- [7] Olalla C., Leyva R., A. El Aroudi, P. Garce's, "LMI robust control design for boost PWM converters", *IET Power Electronics*.
- [8] Carlos A. Torres-Pinzón and Ramon L, "Matlab: a systems tool for design of fuzzy LMI controller in DC-DC converters", 2011.
- [9] Kazuo T., Hua O. W., "Fuzzy Control Systems Design and Analysis: A Linear Matrix Inequality Approach", John Wiley & Sons, Inc., 2001, pp. 259-276.
- [10] Sherer C. and Weiland S., "Linear Matrix Inequalities in Control", 2005.
- [11] Zheng F., Wang Q. G., Lee T. H., "On the design of multivariable PID controllers via LMI approach", *Automatica*, pp. 517-526, 2002.
- [12] Ziegler, J. G. and N. B. Nichols, "Optimum settings for automatic controllers", *Trans. ASME*, 65, 433-444.